Aalborg Universitet

AALBORG
UNIVERSITY

Parametric analysis on the heat transfer, daylight and thermal comfort for a sustainable roof window with triple glazing and external shutter

Liu, Mingzhe; Heiselberg, Per Kvols; Antonov, Yovko Ivanov; Mikkelsen, Frederik Søndergaard

Accepted Manuscript

Parametric analysis on the heat transfer, daylight and thermal comfort for a sustainable roof window with triple glazing and external shutter

Mingzhe Liu , Per Kvols Heiselberg , Yovko Ivanov Antonov , Frederik Søndergaard Mikkelsen
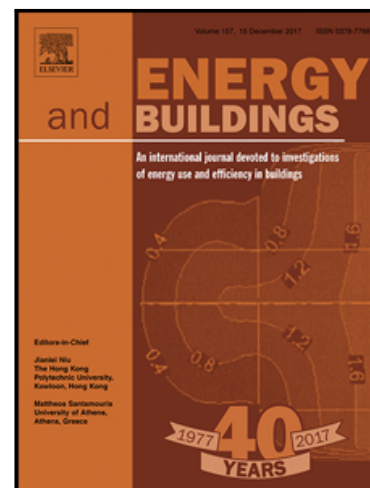
Please cite this article as: Mingzhe Liu ,   Per Kvols Heiselberg ,   Yovko Ivanov Antonov , Frederik Søndergaard Mikkelsen , Parametric analysis on the heat transfer, daylight and thermal comfort for a sustainable roof window with triple glazing and external shutter, *Energy & Buildings* (2018), doi: https://doi.org/10.1016/j.enbuild.2018.11.001

Parametric analysis on the heat transfer, daylight and thermal comfort for a sustainable roof window with triple glazing and external shutter

Mingzhe Liu[a,*], Per Kvols Heiselberg[a], Yovko Ivanov Antonov[a], Frederik Søndergaard Mikkelsen[a]

[a] Department of Civil Engineering, Thomas Manns Vej 23, 9220 Aalborg Ø, Denmark

* Corresponding author. Tel.: +45 99407234.

  E-mail address: ml@civil.aau.dk.

Abstract

Roof windows are widely used in northern European countries, contributing positively by giving daylight, passive solar heat and view to the outside. In order to improve their thermal property, triple glazing unit together with external shutter are more and more common on the market. Additionally, the junction part between window and roof is also important since it greatly influences the linear thermal transmittance (LTT) along edges of the window and the daylight level of the room. This research presents a parametric analysis for roof windows with triple glazing unit and external shutter from perspectives of energy, daylight and thermal comfort. The investigation can be described in two parts:

- Analysis of thermal and comfort performance for triple glazing unit with an external shutter.

- Analysis of combined performance of daylight level and LTT for roof windows.

Performances of energy and thermal comfort of triple glazing unit with external shutter can be influenced by different properties, including the width of the cavity between shutter and external pane, air penetration rate through the cavity between shutter and external pane, the tilt angle of the window. The study conducts analysis on the energy and comfort performances of the window by calculating U-value of the entire window and internal surface temperature of the glazing. The calculations are performed by a model developed via state-space modelling using Simulink/MATLAB. The results reveal that the external shutter improves both the thermal and comfort performances of the window.

The ways of installing windows on a roof and cutting on the internal wall along window edges also have great influences on the combined performance of daylight level and LTT along the edge between window and roof. Therefore, daylight and LTT are also evaluated with different parameters, including the thickness of roof insulation, installation level of windows on the roof, cutting of lining and extra insulation around the perimeter of windows. The analysis is conducted using DIVA/Rhino and Flixo. The calculations show that the lower installation level and extra insulation around the window frame can decrease linear thermal transmittance of the entire window by more than 60 %.

Keywords: roof window, state-space modelling, triple glazing unit, shutter, daylight, linear thermal transmittance, U-value

1. Introduction

The window is a very important building element in need of improvement in order to comply with the requirement of 'nearly zero-energy' in the Energy Performance of Buildings Directive [1]. Roof windows are widely used in northern European countries, contributing positively by giving daylight, passive solar heat and view to the outside. However, a traditional roof window has a higher energy loss through transmission, which can be improved by developing a well-insulated

window with external shutter. Triple glazing units are becoming more and more widely used in modern buildings since they provide better performances of energy and thermal comfort by providing shading in summer and extra insulation in winter. It also protects the window from condensation on the external surface of the glazing. Besides window itself, junction part between window and roof is also important to the linear thermal transmittance (LTT) along the edge of the window and the daylight level behind the window. In order to investigate the performance influenced by different characteristics and provide a better guidance to the design of roof window, it is necessary to conduct a holistic analysis on different parameters to optimize the effects of the window itself (triple glazing with external shutter) and the way it is installed on a roof.

Window shutter is not a recent invention, and different researches have been implemented showing the energy and comfort benefit of using insulation shutter dynamically [2, 3]. Attention has increased for the use of window shutters which reduce heat loss [4-7]. Selkowitz [5] showed that the movable insulation improved both the energy and comfort performance of the façade. It was identified that internal insulating shutters increased the likelihood of condensation and detailed investigations needed to be implemented. Nicol [4] has examined different kinds of window coverings, showing that the movable insulation constructed of 2.5cm beadboard performs better as the internal window shutter. Some studies have investigated the detailed technical issues concerning window shutters [7, 8]. Zaheer-Uddin [7] has found that the heating requirements of houses would increase by 5-10% over houses with perfect shutters because of the dynamic effects. Literatures described before focus on the dynamic performance of window with a shutter on a yearly base. However, performances of the window with external shutters of varying properties under the state of closing need to be detail investigated so that it can provide better performance in the dynamic situation. Yazicioglu has employed comparative analysis of energy performance of traditional wooden shutters and contemporary aluminium roller shutters in Istanbul [9]. Numerical and

experimental validation has been conducted to evaluate thermal transmittance of windows with cellular shades [10]. An experimental study by E.M. Alawadhi et al. [11] has compared heat flux from indoor surface of the window to room depending on the opening of the shutter in a hot climate. However, only one parameter (size of shutter opening) was investigated in the study. It is also interesting to compare internal surface temperature for evaluation of thermal comfort. Numerical and experimental studies by T. Silva et al. [12-14] conclude that a window with internal shutter integrated with PCM could improve indoor thermal comfort in Mediterranean climate during both winter and summer. An external shutter is more interesting for northern European countries since it provides better energy performance and prevents condensation in winter. In summer it is also working as solar shading to prevent overheating. Therefore, it is necessary and interesting to investigate the influence of different parameters of a triple glazing unit with an external shutter in order to optimize the thermal comfort and energy performance.

Another function of roof window is to provide daylight. Since the roof window will be used in northern European countries where roof insulation needs to be thick in order to provide lower U-value, the installation of a roof window on the roof is very important for daylight level in the room and LTT. At this moment, most previous studies separate the performances of daylight level and LTT. Study with application of infrared thermography technique shows that joint between window and construction is equally important as other thermal bridges within windows [15]. Misiopecki et al. [16] investigated thermal bridging effects of window position on different wall constructions. They found out the most efficient window position and concluded that, in some cases, placing the window in the most energy-efficient position reduced LTT over 50 %. Cappelletti et al. carried out analysis of thermal bridges along a wooden frame window installed into two different kinds of external clay block walls [17]. Both of the studies focus on the position of window on the wall, but it is also interesting to evaluate other parameters on the combined performance of daylight and

LTT. Regarding the investigation of daylight level, most studies focus on the influence of glazing of the window instead of the installation of the window on the roof. Jelle et al. [18] have reviewed the existing glazing products and technologies on the market today, identifying some promising fenestration techniques and options. W.J.Hee et al. [19] revealed the impacts of window glazing on the energy and daylighting performances, highlighting the optimization techniques used by various researchers. Gasparella et al. [20] investigated the influence of window size and location for different glazing types, concluding that the demand for space heating can be reduced by large south-orienting windows. Jaber and Ajib came to a similar conclusion that space heating demand was reduced by increasing the size of the south-facing windows [21]. Daylight performance is also investigated by using different type of windows, e.g. electrochromic window and thermochromic window [22, 23], which can lead to energy saving of 19.9 % and daylight performance improvement of 15.5 %. U-value and g value influence the heating and cooling demand in a residential building in northern and southern climate in Korea [24]. Furthermore, Tsikaloudaki et al. [25] also conducted a parametric study on the energy performance of windows to investigate the influence that the thermal and optical properties of glazing have on the cooling demand. Different window cases were also compared on the performance of daylight and thermal comfort [26, 27], which focused more on office buildings. Studies by G.C.J. Skarning et al. [28, 29] investigated the effect of multiple combinations of window size, basic glazing and frame properties on energy, daylight and thermal comfort in nearly zero-energy houses located in Rome and Copenhagen. Different from previous studies, this study focuses on investigating the effects of more parameters related to the window installation on a sloping roof. Additionally, the investigation combines the performances of both linear thermal transmittance and daylight level.

This paper presents a parametric analysis of thermal and comfort performances of triple glazing with external shutter influenced by parameters including tilt angle of the entire window, cavity

thickness between glazing unit and shutter, air penetration rate between the cavity and outdoor air and position of coating on the shutter. Additionally, this study presents an analysis of combined daylight level and LTT of windows influenced by properties such as installation level of the window on the roof, insulation around the window frame, cutting of lining and thickness of roof insulation layer. Due to the requirement of detailed geometric modelling to simulate the daylight level influenced by different installation cases, the modelling and simulations of the daylight level are conducted using DIVA/Rhino [30]. Calculations of LTT of different cases are performed in Flixo [31].

2. Description and research methods

The research can be divided into two parts. The first part is to investigate the performance of the triple glazing unit with external shutter, which is conducted using a dynamic simulation model developed by the authors. The second part is to investigate the combined performance of daylight and linear thermal transmittance using software DIVA/Rhino and Flixo. Detail information about the methods of the two parts is described in this section.

2.1. Calculation and optimization of thermal and comfort performance for triple glazing with an external shutter

In this research, the façades were built with triple glazing unit with an external shutter (**Error! Reference source not found.**). Air and argon is used for the closed cavity between panes since it is common on the market and suggested by Velux. **Error! Reference source not found.** shows types of glass pane and gas used on the triple glazing unit with thermal and solar information. The shutter is movable and working as an insulation layer at night and shading during summer time. When it is closed, there is an air gap between the glazing and the shutter. Air penetration happens between outdoor air and the cavity. The penetration rate depends on the tightness of the shutter and the

connection between the glazing and the shutter, and it could influence thermal and comfort performances of the entire window system. The shutter used in this case is made of aluminium with solar absorption assumed to be 0.85 and emissivity assumed to be 0.85.

In order to optimize the thermal (U-value) and comfort (surface temperature of the internal pane of the window) performances of a triple glazing unit with external shutter, investigations have been conducted on cases with different properties. It needs to be noted that window only influence the thermal comfort as one element in the room. The assumption here is that the thermal properties of the room, e.g. room air temperature, temperatures of other surfaces and other thermal parameters, are the same, leaving window the only changed element in different scenarios. By improving the thermal performance of window and using shutter, the global and local thermal comfort can be improved since the internal surface temperature of window increases in winter and decreases in summer.

These investigations evaluate the influence of parameters shown in **Error! Reference source not found.**, including a variation of the tilt angle, air penetration rate of the cavity, the position of coating on the shutter and thickness of cavity between the shutter and glazing, etc. The calculations are performed in a state space modelling of triple glazing unit with an external shutter (which is described later on) considering the boundary conditions in Table 3. The temperatures in the boundary conditions are according to the standards ISO 15099 [32]. However, instead of using the number from the standard, lower solar radiation in winter (0 W/m^2) and higher solar radiation in summer (700 W/m^2) are used in the boundary conditions to assess the performance in a harsh environment.

2.1.1. State space modelling for triple glazing unit with an external shutter

Numerical simulations are conducted to calculate the U-value and the internal surface temperature of a window with triple glazing and external shutter. The model is developed by extending an existing method which has been verified by [2, 33, 34] and been used to simulate dynamic façade [3, 35]. The model has been verified by simulation tool WINDOW 7.4 developed by Lawrence Berkeley National Laboratory [36].

The model is implemented by building finite element energy balance equations according to the RC model, in which the external pane, the central pane and the internal pane are divided into two nodes, respectively (**Error! Reference source not found.**). Simulink is used to build and calculate the model. The external shutter and the cavity between the shutter and external pane are also considered as one node each. It is assumed that each node is homogeneous with the same temperature. Equations 1 to 8 shown below are built according to the energy balance of the eight nodes.

Equations 1 and 2 describe the heat balance of nodes of the external shutter and the cavity between shutter and external pane. Equations 3 and 4 describe the heat balance of nodes on the external pane. Equations 5 and 6 describe heat balance of nodes on the central pane. Equations 7 and 8 describe the heat balance of nodes on the internal pane.

$$\frac{dT_{sh}}{dt} C_{sh} m_{sh} = (T_o - T_{sh}) \times h_{c\_e} + (T_{sky} - T_{sh}) \times h_{r\_e} + (T_{e1} - T_{sh}) \times h_{r\_sg} + (T_{ca} - T_{sh}) \times h_{\text{cov}\_ca} + \phi_{sol\_sh} \tag{1}$$

$$\frac{dT_{ca}}{dt} C_{ca} m_{ca} = (T_{sh} - T_{ca}) \times h_{\text{cov}\_ca} + (T_{e1} - T_{ca}) \times h_{\text{cov}\_ca} + (T_o - T_{ca}) \times h_{\text{inf}\_ca} \tag{2}$$

$$\frac{dT_{e1}}{dt} C_{e1} m_{e1} = (T_{ca} - T_{e1}) \times h_{\text{cov}\_ca} + (T_{sh} - T_{e1}) \times h_{r\_sg} + (T_{e2} - T_{e1}) \times h_{con\_e} \tag{3}$$

$$\frac{dT_{e2}}{dt} C_{e2} m_{e2} = (T_{e1} - T_{e2}) \times h_{con\_e} + (T_{c1} - T_{e2}) \times h_{cov\_ec} + (T_{c1} - T_{e2}) \times h_{r\_ec} \qquad (4)$$

$$\frac{dT_{c1}}{dt} C_{c1} m_{c1} = (T_{e2} - T_{c1}) \times h_{cov\_ec} + (T_{e2} - T_{c1}) \times h_{r\_ec} + (T_{c2} - T_{c1}) \times h_{con\_c} \qquad (5)$$

$$\frac{dT_{c2}}{dt} C_{c2} m_{c2} = (T_{c1} - T_{c2}) \times h_{con\_c} + (T_{i1} - T_{c2}) \times h_{cov\_ci} + (T_{i1} - T_{c2}) \times h_{r\_ci} \qquad (6)$$

$$\frac{dT_{i1}}{dt} C_{i1} m_{i1} = (T_{c2} - T_{i1}) \times h_{cov\_ci} + (T_{i2} - T_{i1}) \times h_{con\_i} + (T_{c2} - T_{i1}) \times h_{r\_ci} \qquad (7)$$

$$\frac{dT_{i2}}{dt} C_{i2} m_{i2} = (T_i - T_{i2}) \times h_{c\_i} + (T_s - T_{i2}) \times h_{r\_i} + (T_{i1} - T_{i2}) \times h_{con\_i} \qquad (8)$$

Parameters used in the equations are as follows:

T_{sh} and T_{ca} are temperatures of the external shutter and the air cavity between the external shutter and the external pane. T_{e1} and T_{oi} are temperatures of the external and internal nodes of the external pane. T_{c1} and T_{c2} are temperatures of the external and internal nodes of the central pane; T_{i1} and T_{i2} are temperatures of the external and internal nodes of the internal panes; C_{sh}, C_{ca}, C_{e1}, C_{e2}, C_{c1}, C_{c2}, C_{i1}, and C_{i2} are the heat capacity of the eight nodes from outside to inside; m_{sh}, m_{ca}, m_{oe}, m_{om}, m_{oi}, m_{ce}, m_{cm}, m_{ci}, m_{ie}, m_{im} and m_{ii} are the weight of the eight nodes from outside to inside; Φ_{sol_sh} is the solar absorption on the node of the external shutter; h_{c_e}, h_{c_i}, h_{r_e}, and h_{r_i}, are exterior and interior convective and radiative heat transfer coefficient, which are calculated according to [2].

Input information is indoor wall surface temperature T_s, indoor and outdoor air temperatures T_i and T_o. Outdoor surrounding equivalent temperature T_{sky} is calculated according to the outdoor air temperature T_o [2]. Furthermore, convective and radiative heat transfer coefficients are calculated according to Clarke [37]. Convective heat transfer coefficient in the cavity and radiative heat transfer coefficient between the two panes are described in EN 673 [38]. It needs to be noted that new experimental research in [39] shows that actual U-value is higher than theoretical data and

concludes that thermal bridges and edge effects play a key role in actual U-value performance of glazing product. However, there is no method that is concluded and can be used in the model of this paper.

Equations 1 to 8 can be rewritten as equations 9 to 16 shown below:

$$\frac{dT_{sh}}{dt} = \frac{-\left(h_{\text{cov}\_ca} + h_{r\_sg} + h_{c\_e} + h_{r\_e}\right)}{C_{sh}m_{sh}} \times T_{sh} + \frac{h_{\text{cov}\_ca}}{C_{sh}m_{sh}} \times T_{ca} + \frac{h_{r\_sg}}{C_{sh}m_{sh}} \times T_{e1} + \frac{h_{c\_e}}{C_{sh}m_{sh}} \times T_o + \frac{h_{r\_e}}{C_{sh}m_{sh}} \times T_{sky} + \frac{1}{C_{sh}m_{sh}} \times \phi_{sol\_sh}$$
(9)

$$\frac{dT_{ca}}{dt} = \frac{-\left(h_{\text{cov}\_ca} + h_{\text{cov}\_ca} + h_{\text{inf}\_ca}\right)}{C_{ca}m_{ca}} \times T_{ca} + \frac{h_{\text{cov}\_ca}}{C_{ca}m_{ca}} \times T_{sh} + \frac{h_{\text{cov}\_ca}}{C_{ca}m_{ca}} \times T_{e1} + \frac{h_{\text{inf}\_ca}}{C_{ca}m_{ca}} \times T_o \qquad \textbf{(10)}$$

$$\frac{dT_{e1}}{dt} = \frac{-\left(h_{con\_e} + h_{r\_sg} + h_{\text{cov}\_ca}\right)}{C_{e1}m_{e1}} \times T_{e1} + \frac{h_{con\_e}}{C_{e1}m_{e1}} \times T_{e2} + \frac{h_{r\_sg}}{C_{e1}m_{e1}} \times T_{sh} + \frac{h_{\text{cov}\_ca}}{C_{e1}m_{e1}} \times T_{ca} \qquad \textbf{(11)}$$

$$\frac{dT_{e2}}{dt} = \frac{-\left(h_{con\_e} + h_{\text{cov}\_ec} + h_{r\_ec}\right)}{C_{e2}m_{e2}} \times T_{e2} + \frac{h_{con\_e}}{C_{e2}m_{e2}} \times T_{e1} + \frac{\left(h_{\text{cov}\_ec} + h_{r\_ec}\right)}{C_{e2}m_{e2}} \times T_{c1} \qquad \textbf{(12)}$$

$$\frac{dT_{c1}}{dt} = \frac{-\left(h_{\text{cov}\_ec} + h_{con\_c} + h_{r\_ec}\right)}{C_{c1}m_{c1}} \times T_{c1} + \frac{\left(h_{\text{cov}\_ec} + h_{r\_ec}\right)}{C_{c1}m_{c1}} \times T_{e2} + \frac{h_{con\_c}}{C_{c1}m_{c1}} \times T_{c2} \qquad \textbf{(13)}$$

$$\frac{dT_{c2}}{dt} = \frac{-\left(h_{con\_c} + h_{\text{cov}\_ci} + h_{r\_ci}\right)}{C_{c2}m_{c2}} \times T_{c2} + \frac{h_{con\_c}}{C_{c2}m_{c2}} \times T_{c1} + \frac{\left(h_{\text{cov}\_ci} + h_{r\_ci}\right)}{C_{c2}m_{c2}} \times T_{i1} \qquad \textbf{(14)}$$

$$\frac{dT_{i1}}{dt} = \frac{-\left(h_{con\_i} + h_{\text{cov}\_ci} + h_{r\_ci}\right)}{C_{i1}m_{i1}} \times T_{i1} + \frac{\left(h_{\text{cov}\_ci} + h_{r\_ci}\right)}{C_{i1}m_{i1}} \times T_{c2} + \frac{h_{con\_i}}{C_{i1}m_{i1}} \times T_{i2} \qquad \textbf{(15)}$$

$$\frac{dT_{i2}}{dt} = \frac{-\left(h_{con\_i} + h_{c\_i} + h_{r\_i}\right)}{C_{i2}m_{i2}} \times T_{i2} + \frac{h_{con\_i}}{C_{i2}m_{i2}} \times T_{i1} + \frac{h_{c\_i}}{C_{i2}m_{i2}} \times T_i + \frac{h_{r\_i}}{C_{i2}m_{i2}} \times T_s \qquad \textbf{(16)}$$

State-space modelling is used in this study to build and solve the heat balance equations into two equations of matrixes (equation 17).

$$\dot{T} = A \cdot T + B \cdot U$$
$$T = C \cdot T + D \cdot U$$

(17)

T, which is a matrix of temperatures variables of the eight nodes, can be calculated by inputting matrixes of parameters A, B, C, D and matrix of input U into Simulink. In order to make it clear, variables of matrixes T is marked with red colour, and variables of matrix U are marked with the colour blue in equations 9 to 16. Matrixes T, A, B, C, D and U are shown in equations 18 to 23.

$$
A = \begin{bmatrix}
\dfrac{-(h_{cov\_ca} + h_{r\_sg} + h_{c\_e} + h_{r\_e})}{C_{sh}m_{sh}} & \dfrac{h_{cov\_ca}}{C_{sh}m_{sh}} & \dfrac{h_{r\_sg}}{C_{sh}m_{sh}} & 0 & 0 & 0 \\[3mm]
\dfrac{h_{cov\_ca}}{C_{ca}m_{ca}} & \dfrac{-(h_{cov\_ca} + h_{cov\_ca} + h_{inf\_ca})}{C_{ca}m_{ca}} & \dfrac{h_{cov\_ca}}{C_{ca}m_{ca}} & 0 & 0 & 0 \\[3mm]
\dfrac{h_{r\_sg}}{C_{e1}m_{e1}} & \dfrac{h_{cov\_ca}}{C_{e1}m_{e1}} & \dfrac{-(h_{con\_e} + h_{r\_sg} + h_{cov\_ca})}{C_{e1}m_{e1}} & \dfrac{h_{con\_e}}{C_{e1}m_{e1}} & 0 & 0 \\[3mm]
0 & 0 & \dfrac{h_{con\_e}}{C_{e2}m_{e2}} & \dfrac{-(h_{con\_e} + h_{cov\_ec} + h_{r\_ec})}{C_{e2}m_{e2}} & \dfrac{(h_{cov\_ec} + h_{r\_ec})}{C_{e2}m_{e2}} & 0 \\[3mm]
0 & 0 & 0 & \dfrac{(h_{cov\_ec} + h_{r\_ec})}{C_{c1}m_{c1}} & \dfrac{-(h_{cov\_ec} + h_{con\_c} + h_{r\_ec})}{C_{c1}m_{c1}} & \dfrac{h_{con\_c}}{C_{c1}m_{c1}} \\[3mm]
0 & 0 & 0 & 0 & \dfrac{h_{con\_c}}{C_{c2}m_{c2}} & \dfrac{-(h_{con\_c} + h_{cov\_ci} + h_{r\_ci})}{C_{c2}m_{c2}} \\[3mm]
0 & 0 & 0 & 0 & 0 & \dfrac{(h_{cov\_ci} + h_{r\_ci})}{C_{i1}m_{i1}} & -\left(h_{c...}\right) \\[3mm]
0 & 0 & 0 & 0 & 0 & 0
\end{bmatrix}
$$

(18)

$$
B = \begin{bmatrix}
\dfrac{h_{c\_e}}{C_{sh}m_{sh}} & \dfrac{h_{r\_e}}{C_{sh}m_{sh}} & \dfrac{1}{C_{sh}m_{sh}} & 0 & 0 \\[3mm]
\dfrac{h_{inf\_ca}}{C_{ca}m_{ca}} & 0 & 0 & 0 & 0 \\[3mm]
0 & 0 & 0 & 0 & 0 \\[3mm]
0 & 0 & 0 & 0 & 0 \\[3mm]
0 & 0 & 0 & 0 & 0 \\[3mm]
0 & 0 & 0 & 0 & 0 \\[3mm]
0 & 0 & 0 & 0 & 0 \\[3mm]
0 & 0 & 0 & \dfrac{h_{c\_i}}{C_{i2}m_{i2}} & \dfrac{h_{r\_i}}{C_{i2}m_{i2}}
\end{bmatrix}
$$

(19)

$$C = \begin{bmatrix} 1 & 0 & 0 & 0 & 0 & 0 & 0 & 0 \\ 0 & 1 & 0 & 0 & 0 & 0 & 0 & 0 \\ 0 & 0 & 1 & 0 & 0 & 0 & 0 & 0 \\ 0 & 0 & 0 & 1 & 0 & 0 & 0 & 0 \\ 0 & 0 & 0 & 0 & 1 & 0 & 0 & 0 \\ 0 & 0 & 0 & 0 & 0 & 1 & 0 & 0 \\ 0 & 0 & 0 & 0 & 0 & 0 & 1 & 0 \\ 0 & 0 & 0 & 0 & 0 & 0 & 0 & 1 \end{bmatrix} \quad \text{(20)}$$

$$D = \begin{bmatrix} 0 & 0 & 0 & 0 & 0 \\ 0 & 0 & 0 & 0 & 0 \\ 0 & 0 & 0 & 0 & 0 \\ 0 & 0 & 0 & 0 & 0 \\ 0 & 0 & 0 & 0 & 0 \\ 0 & 0 & 0 & 0 & 0 \\ 0 & 0 & 0 & 0 & 0 \\ 0 & 0 & 0 & 0 & 0 \end{bmatrix} \quad \text{(21)}$$

$$T = \begin{bmatrix} T_{sh} \\ T_{ca} \\ T_{e1} \\ T_{e2} \\ T_{c1} \\ T_{c2} \\ T_{i1} \\ T_{i2} \end{bmatrix} \quad \text{(22)}$$

$$U = \begin{bmatrix} T_o \\ T_{sky} \\ \Phi_{sol\_sh} \\ T_i \\ T_s \end{bmatrix} \quad \text{(23)}$$

2.2. Simulation and analysis of daylight level and LTT for different installation cases

Daylight level and LTT along the edges between the window and roof are influenced by different parameters related to windows installation on a sloping roof (45 degrees). In order to evaluate the influences, simulations have been conducted to compare the combined performance of daylight level in a room and LTT through a window for different installation cases. **Error! Reference source not found.** shows the variant parameters of the installation cases, including the thickness of roof insulation, installation level of the window, lining cutting of roof and extra insulation around the window frame. Simulations are performed with combinations of different parameters in each case (810 combinations in total). It needs to be noted that cuttings on side lining are only implemented for cases with the insulation thicknesses of 350 mm and 550 mm since the cases of 150 mm are too thin to be cut.

Error! Reference source not found. to **Error! Reference source not found.** show the schematic drawings of different installation cases. Cases with different insulation thicknesses on the roof (**Error! Reference source not found.**) is determined due to the possible roof insulation in the west and northern Europe, covering Denmark, Sweden, Finland, Norway, Germany, the Netherlands, UK, and Belgium, etc. Different from standard installation level, the performance of possible cases of lowering the installation level with 40 mm and 60 mm are also investigated in this study (**Error! Reference source not found.**). It is similar to the principle in the study conducted by Misiopecki et al. [16]. **Error! Reference source not found.** and **Error! Reference source not found.** show how the windows are installed with different cases of lining cutting. Three cases for top and bottom cutting (**Error! Reference source not found.**) and two cases (**Error! Reference source not found.**) for side cutting are illustrated. Extra insulation can also be added around the perimeter of the

window frame to decrease the LTT along window frame. Six cases are shown in **Error! Reference source not found.** regarding the cases of extra insulation.

Simulations are conducted using DIVA/Rhino [30] and Flixo [31]. DIVA is dynamic software which can be plugged into Rhino and is capable of simulating static and dynamic daylight metrics. The choice of DIVA/Rhino is determined since the investigated cases require simulation for detail and complex geometry. The results are presented using Matlab. The calculated performance of daylight level and LTT are as follows:

- Relative floor area above daylight criteria (daylight factor of 2 %), [%]
- Total LTT of the entire window (size of 1140 mm*1340 mm), [W/K]

3. Result

3.1. Thermal and comfort performance of triple glazing with external shutter

Calculation results of thermal performance of different cases in **Error! Reference source not found.** are shown in **Error! Reference source not found.**. Based on the results, it is shown that total U-value of the window with an external shutter is decreased as the window rotates from a vertical position to horizontal position (different markers in the figure: 'x', 'o' and '-'). It can be explained by the differences of view factors between window and sky and convective heat transfer in the cavity due to different positions. The difference can be as high as 0.3 W/(m²·K).

It is also clearly shown the difference of U-value because of the different position of coating on the shutter. The U-value is decreased by more than 30 % with the help of implementing low-E coating on both sides of the shutter compared with shutter without any coating. Cases with internal coating perform better than that with external coating.

The increase of air penetration rate increases the U-value of all the cases except cases without any coating on the shutter. U-value of the cases without coating slightly decrease as the increase of air penetration rate, which can be explained that higher air penetration rate helps heat up the shutter with external air if the temperature of the shutter is too low due to the radiative heat transfer to the sky. This situation might be different as for a change of boundary condition (clear sky or cloudy sky).

It is also seen from the figure that the cavity thickness between glazing and shutter influences the U-value differently for different inclination cases. For cases of vertical position ('x'), the U-value decreases first and then increases as the cavity thickness increases. The cases with the cavity thickness of 20 mm have lower U-value than other cases. The U-value can be decreased by 10 % if the cavity thickness is increased from 10 mm to 20 mm. The results of the horizontal cases ('o') have a reverse trend as the vertical cases, resulting in the highest U-value on cavity thickness of 15 mm. Results of the cases of 45 degrees ('-') are more complicated than the other two groups. Lower U-value can be found when the cavity thickness is 15 mm or 50 mm (maybe even thicker according to the trend, but the calculation is conducted until 50 mm). The different trends in the results of different inclination cases are combined effects of convection, conduction and long-wave radiation due to different inclination angles. Furthermore, the trends are independent of air penetration rate through the cavity.

The thermal comfort of different cases is investigated in summer condition in terms of surface temperature of the internal pane (**Error! Reference source not found.**). The surface temperature of triple glazing window without shutter is also calculated as a reference, which is 34 °C. Therefore, it

is clear that the shutter works as solar shading and improves the thermal comfort level in summer by decreasing surface temperature of the internal pane to the range between 25.9 °C and 28.2 °C depending on different cases. It is obvious that the increase in air penetration rate decreases the surface temperature since it cools down the cavity with outdoor air. It can also be concluded that external coating on the shutter increases the surface temperature since it decreases the radiative heat loss from the shutter to the sky. The internal coating effects differently because it decreases the transfer of absorbed heat by the shutter to the glazing unit. The fact that the surface temperatures of vertical cases are lower than the horizontal and 45 degrees corresponds to the results of U-value. The lower U-value decreases heat transfer from the shutter to the internal surface in summer condition, maintaining lower internal surface temperature.

The temperature in the cavity is also calculated in summer condition for different cases in order to investigate the risk of overheating in the cavity which is important to the durability of the materials exposed to the cavity. **Error! Reference source not found.** shows that the highest air temperature in the cavity between shutter and external pane is less than 50 °C even for the cases without any air penetration.

3.2. Combined performance of daylight and LTT of different installation cases

This section presents the combined performance of daylight and LTT of different installation cases of roof window.

A lower installation level improves both daylight level and thermal performance (**Error! Reference source not found.**). The floor area with daylight level above criteria is increased by 1 % as the window position is moved from cases 0 mm to cases -60 mm. The mean LTT value of the entire window drops from 0.58 W/K to 0.3 W/K as the cases move from 0 mm to -60 mm due to the reduction of the area of window perimeter exposed to the outdoor condition. The results also correspond to what has been found by Misiopecki et al. [16] that the LTT can be decreased by 50 % by moving windows to an optimal position.

Extra insulation around window frame will decrease LTT, which is presented in **Error! Reference source not found.**. The boxplot shows the LTT as the function of different cases of extra insulation from 'T1 0/T2 0' to 'T1 60/T2 60'. Detail drawings of the cases are shown in **Error! Reference source not found.**. The three lines with different types present the mean LTT values of different position cases (0 mm, -40 mm and -60 mm) within each case of extra insulation. It can be seen from the boxplot that the general trend of linear thermal transmittance is to decrease from all the cases of 'T1 0/T2 0' to all the cases of 'T1 60/T2 60', which is because that more insulation around the perimeter of window frame decreases heat loss. One exception is shown by the solid line (case of 0 mm) that the LTT slightly increases from the cases of 'T1 30/T2 30' to the cases of 'T1 60/T2 0'. It means that, for cases of 0 mm, a higher but thinner insulation ('T1 30/T2 30') is better than a lower but thicker insulation ('T1 60/T2 0'). The extra insulation does not influence daylight level since it is outside the window installation perimeter.

Error! Reference source not found. and **Error! Reference source not found.** present the daylight level and LTT influenced by the thickness of roof insulation and lining cutting.

It reveals (**Error! Reference source not found.**) that the daylight level decreases significantly as the thickness of roof insulation increases. The relative floor area above the daylight criteria decreases from 37 % to 28 % as the roof insulation increases from 150 mm to 550 mm. It can also be seen that the lining cutting on top and bottom improves the daylight level for all the cases (150 mm, 350 mm and 550 mm). However, the improvement for 550 mm is smaller than that for 150 mm and 350 mm. For cases of 350 mm and cases of 550 mm, lining cutting on the left and right sides of the window is also implemented and simulated. The results show that cutting on the left and right sides (colour green in the figure) and cutting on all the sides around the window (colour black in the figure) improve the daylight performance even further. For cases of 550 mm, the effect of the cutting on left and right sides is much more obvious than that of 350 mm. In addition, cutting all sides (top, bottom and sides) has almost the same daylight level as cutting on two sides for the case of 550 mm.

A drawback of the lining cuttings is the increase of LTT through window installation, especially for cutting on top and bottom (**Error! Reference source not found.**). The results of LTT also increase as the insulation thickness increases, which can be explained that more heat will be transferred through window frame when it is difficult to be transferred through roof insulation.

4. Conclusion

Different parameters have been investigated for triple glazing with external shutter and installation of roof window in order to optimize the performances of energy, thermal comfort and daylight level. By using an external shutter, it is possible to reduce heat loss of windows in winter and improve the indoor comfort performance in summer.

Total U-value of the window with external shutter can be decreased by as high as 0.3 W/(m²·K) as the window rotates from vertical position to horizontal position. The increase of air penetration rate increases the U-value of all the cases except cases without any coating on the shutter. U-value is lower when the thickness of the cavity between shutter and external pane is around 20 mm for vertical window and window of 45 degrees. However, the performance is better when the cavity is much thicker (50 mm) for horizontal window. In addition, it is better to implement coating at least on the internal side of the shutter to reduce the radiative heat transfer. The U-value can be decreased by more than 30 % with the help of implementing low-E coating on both sides of the shutter compared with shutter without any coating.

The surface temperature of internal pane can be decreased from 34 °C to the range between 25.9 °C and 28.2 °C in summer by implementing external shutter. Higher air penetration rate between the cavity and outdoor environment decreases air temperature in the cavity and surface temperature on the internal pane.

The relative floor area above the daylight criteria decreases from 37 % to 28 % as the roof insulation increases from 150 mm to 550 mm. Side cutting performs better than top and bottom cutting in terms of daylight level, especially for thick roof insulation (550 mm). Lower installation level and extra insulation around the window frame can decrease linear thermal transmittance of the entire window by more than 60 %.

As the guidance for future design, the conclusions of this study are as follows:

- It is recommended to have the shutter with coating on either both sides or internal side to have better thermal and comfort performance.

- It is recommended to have extra insulation of 'T1 60 mm T2 60 mm' around the perimeter of a roof window to decrease the LTT.

- It is recommended to lower the installation position to -60 mm to improve both the performances of LTT and daylight.

- It is recommended to conduct the internal lining cuttings either on all sides (top, bottom, left and right sides) or on left and right sides of the window to improve daylight level.

Nomenclature

T_{sh} temperature of external shutter [°C];

T_{ca} air temperature of the cavity between external shutter and external pane [°C];

T_{e1} temperature of external node of the external pane [°C];

T_{e2} temperature of internal node of the external pane [°C];

T_{c1} temperature of external node of the gas cavity [°C];

T_{c2} temperature of internal node of the gas cavity [°C];

T_{i1} temperature of external node of the internal pane [°C];

T_{i2} temperature of internal node of the internal pane [°C];

C_{sh} heat capacity of external shutter [J/(kg·K)];

C_{ca} heat capacity of the air between external shutter and external pane [J/(kg·K)];

C_{e1} heat capacity of external node of the external pane [J/(kg·K)];

C_{e2} heat capacity of internal node of the external pane [J/(kg·K)];

C_{c1} heat capacity of external node of the gas cavity [J/(kg·K)];

C_{c2} heat capacity of internal node of the gas cavity [J/(kg·K)];

C_{i1} heat capacity of external node of the internal pane [J/(kg·K)];

C_{i2} heat capacity of internal node of the internal pane [J/(kg·K)];

m_{sh} weight of external shutter [kg];

m_{ca} weight of the air between external shutter and external pane [kg];

m_{e1} weight of external node of the external pane [kg];

m_{e2} weight of internal node of the external pane [kg];

m_{c1} weight of external node of the gas cavity [kg];

m_{c2} weight of internal node of the gas cavity [kg];

m_{i1} weight of external node of the internal pane [kg];

m_{i2} weight of internal node of the internal pane [kg];

T_i indoor air temperature [°C];

T_o outdoor air temperature [°C];

T_s indoor equivalent surface temperature [°C];

T_{sky} sky temperature [°C];

h_{c_e} external convective heat transfer coefficient [W/(m²·K)];

h_{c_i} internal convective heat transfer coefficient [W/(m²·K)];

h_{r_i} indoor radiative heat transfer coefficient [W/(m²·K)];

h_{r_e} outdoor radiative heat transfer coefficient [W/(m²·K)];

h_{cov_ca} convective heat transfer coefficient in the cavity between external shutter and external pane [W/(m²·K)];

h_{r_sg} radiative heat transfer coefficient between external shutter and external pane [W/(m²·K)];

h_{inf_ca} heat transfer coefficient by air penetration between outdoor and the cavity between external shutter and external pane [W/(m²·K)];

h_{con_e} conductive heat transfer coefficient between nodes on the external pane [W/(m²·K)];

h_{con_c} conductive heat transfer coefficient between nodes on the central pane [W/(m²·K)];

h_{con_i} conductive heat transfer coefficient between nodes on the internal pane [W/(m²·K)];

h_{cov_ec} convective heat transfer coefficient in the cavity between external pane and central pane [W/(m²·K)];

h_{cov_ci} convective heat transfer coefficient in the cavity between central pane and internal pane [W/(m²·K)];

h_{r_ec} radiative heat transfer coefficient in the cavity between external pane and central pane [W/(m²·K)];

h_{r_ci} radiative heat transfer coefficient in the cavity between central pane and internal pane [W/(m²·K)];

Φ_{sol_sh} solar absorption on external shutter [W/m²];

dt   time steps [s];

Acknowledgements

References

[1] a.C. European Parliament, Directive 2010/31/EU on the energy performance of buildings (recast) - 19 May 2010 (2010).

[2] M. Liu, K.B. Wittchen, P.K. Heiselberg, F.V. Winther, Development of a simplified and dynamic method for double glazing façade with night insulation and validated by full-scale façade element, Energy Build. 58 (2013) 163-171.

[3] M. Liu, K.B. Wittchen, P.K. Heiselberg, Control strategies for intelligent glazed façade and their influence on energy and comfort performance of office buildings in Denmark, Appl. Energy. 145 (2015) 43-51.

[4] K. Nicol, The thermal effectiveness of various types of window coverings, Energy Build. 9 (1986) 231-237.

[5] S.E. Selkowitz, Thermal performance of insulating window systems, Lawrence Berkeley National Laboratory (2011).

[6] M. Zaheer-Uddin, The influence of automated window shutters on the design and performance of a passive solar house, Build. Environ. 22 (1987) 67-75.

[7] M. Zaheer-Uddin, Dynamic effects of thermal shutters, Build. Environ. 25 (1990) 33-35.

[8] M. Zaheer-Uddin, The influence of automated window shutters on the design and performance of a passive solar house, Build. Environ. 22 (1987) 67-75.

[9] F. Yazicioglu, A Comparative Analysis of the Energy Performance of Traditional Wooden Shutters and Contemporary Aluminium Roller Shutters in Istanbul, a Case Study, Energy Procedia. 42 (2013) 483-492.

[10] R. Hart, Numerical and experimental validation for the thermal transmittance of windows with cellular shades, Energy and Buildings. 166 (2018) 358-371.

[11] E.M. Alawadhi, Effect of an incompletely closed window shutter on indoor illuminance level and heat gain, Energy Build. 110 (2016) 112-119.

[12] T. Silva, R. Vicente, F. Rodrigues, A. Samagaio, C. Cardoso, Development of a window shutter with phase change materials: Full scale outdoor experimental approach, Energy Build. 88 (2015) 110-121.

[13] T. Silva, R. Vicente, F. Rodrigues, A. Samagaio, C. Cardoso, Performance of a window shutter with phase change material under summer Mediterranean climate conditions, Appl. Therm. Eng. 84 (2015) 246-256.

[14] T. Silva, R. Vicente, C. Amaral, A. Figueiredo, Thermal performance of a window shutter containing PCM: Numerical validation and experimental analysis, Appl. Energy. 179 (2016) 64-84.

[15] M. O'Grady, A.A. Lechowska, A.M. Harte, Application of infrared thermography technique to the thermal assessment of multiple thermal bridges and windows, Energy and Buildings. 168 (2018) 347-362.

[16] C. Misiopecki, M. Bouquin, A. Gustavsen, B.P. Jelle, Thermal modeling and investigation of the most energy-efficient window position, Energy and Buildings. 158 (2018) 1079-1086.

[17] F. Cappelletti, A. Gasparella, P. Romagnoni, P. Baggio, Analysis of the influence of installation thermal bridges on windows performance: The case of clay block walls, Energy and Buildings. 43 (2011) 1435-1442.

[18] B.P. Jelle, A. Hynd, A. Gustavsen, D. Arasteh, H. Goudey, R. Hart, Fenestration of today and tomorrow: A state-of-the-art review and future research opportunities, Solar Energy Mater. Solar Cells. 96 (2012) 1-28.

[19] W. Hee, M. Alghoul, B. Bakhtyar, O. Elayeb, M. Shameri, M. Alrubaih, K. Sopian, The role of window glazing on daylighting and energy saving in buildings, Renewable and Sustainable Energy Reviews. 42 (2015) 323-343.

[20] A. Gasparella, G. Pernigotto, F. Cappelletti, P. Romagnoni, P. Baggio, Analysis and modelling of window and glazing systems energy performance for a well insulated residential building, Energy Build. 43 (2011) 1030-1037.

[21] S. Jaber, S. Ajib, Thermal and economic windows design for different climate zones, Energy Build. 43 (2011) 3208-3215.

[22] J. Dussault, L. Gosselin, Office buildings with electrochromic windows: A sensitivity analysis of design parameters on energy performance, and thermal and visual comfort, Energy and Buildings. 153 (2017) 50-62.

[23] R. Liang, Y. Sun, M. Aburas, R. Wilson, Y. Wu, Evaluation of the thermal and optical performance of thermochromic windows for office buildings in China, Energy and Buildings. 176 (2018) 216-231.

[24] P. Ihm, L. Park, M. Krarti, D. Seo, Impact of window selection on the energy performance of residential buildings in South Korea, Energy Policy. 44 (2012) 1-9.

[25] K. Tsikaloudaki, K. Laskos, T. Theodosiou, D. Bikas, The energy performance of windows in Mediterranean regions, Energy Build. 92 (2015) 180-187.

[26] C.E. Ochoa, M.B. Aries, E.J. van Loenen, J.L. Hensen, Considerations on design optimization criteria for windows providing low energy consumption and high visual comfort, Appl. Energy. 95 (2012) 238-245.

[27] J. Lee, H. Jung, J. Park, J. Lee, Y. Yoon, Optimization of building window system in Asian regions by analyzing solar heat gain and daylighting elements, Renewable Energy. 50 (2013) 522-531.

[28] G.C.J. Skarning, C.A. Hviid, S. Svendsen, Roadmap for improving roof and façade windows in nearly zero-energy houses in Europe, Energy Build. 116 (2016) 602-613.

[29] L. Vanhoutteghem, G.C.J. Skarning, C.A. Hviid, S. Svendsen, Impact of façade window design on energy, daylighting and thermal comfort in nearly zero-energy houses, Energy Build. 102 (2015) 149-156.

[30] http://diva4rhino.com/, DIVA for Rhino, Daylighting and energy modeling plug-in.

[31] http://www.flixo.com/products/flixo-energy/, Thermal bridges for energy performance calculation.

[32] I. ISO, 15099. 2003. Thermal performance of windows, doors and shading devices–detailed calculations, International Organization for Standardization (2003).

[33] M. Liu, K.B. Wittchen, P.K. Heiselberg, Development of a simplified method for intelligent glazed façade design under different control strategies and verified by building simulation tool BSim, Build. Environ. 74 (2014) 31-38.

[34] M. Liu, K.B. Wittchen, P.K. Heiselberg, Verification of a simplified method for intelligent glazed façade design under different control strategies in a full-scale façade test facility–Preliminary

results of a south facing single zone experiment for a limited summer period, Build. Environ. 82 (2014) 400-407.

[35] M. Liu, K.B. Wittchen, P.K. Heiselberg, F.V. Winther, Development and sensitivity study of a simplified and dynamic method for double glazing facade and verified by a full-scale façade element, Energy Build. 68 (2014) 432-443.

[36] R. Mitchell, C. Kohler, L. Zhu, D. Arasteh, J. Carmody, C. Huizenga, D. Curcija, , January."THERM 6.3/WINDOW 6.3 NFRC Simulation Manual." (2011).

[37] J.A. Clarke, Energy simulation in building design, Routledge, 2001.

[38] B. EN, 673: 1998 Glass in building-Determination of thermal transmittance (U value)– Calculation method, British Standards Institution, London, ISBN. 580 (1998) 8.

[39] E. Cuce, Accurate and reliable U-value assessment of argon-filled double glazed windows: A numerical and experimental investigation, Energy and Buildings. 171 (2018) 100-106.

Figures captions
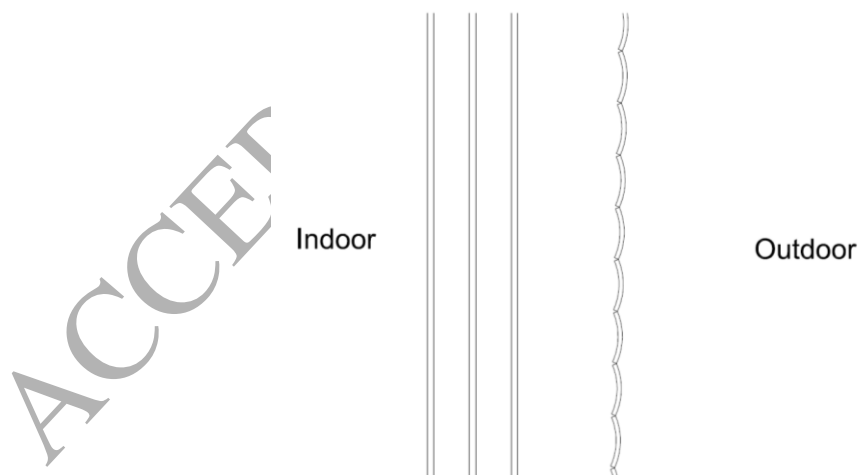
Figure 1: Illustrations of the facades with an external shutter.
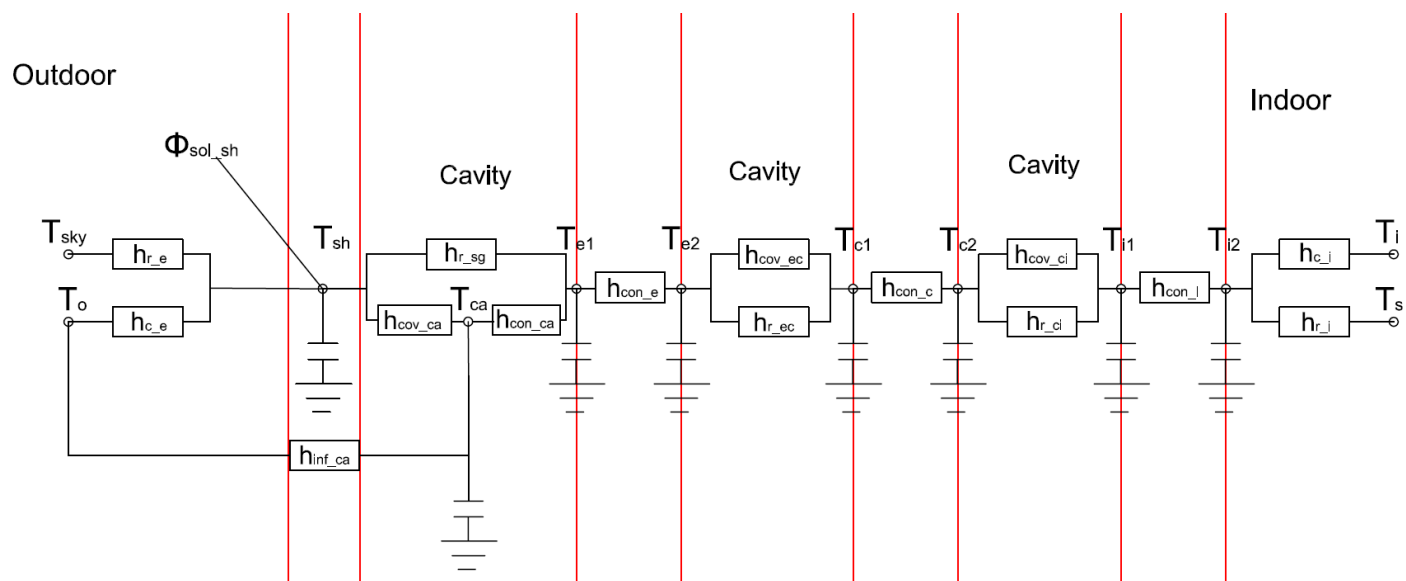
Figure 2: Demonstration of RC network of triple glazing unit with external shutter.
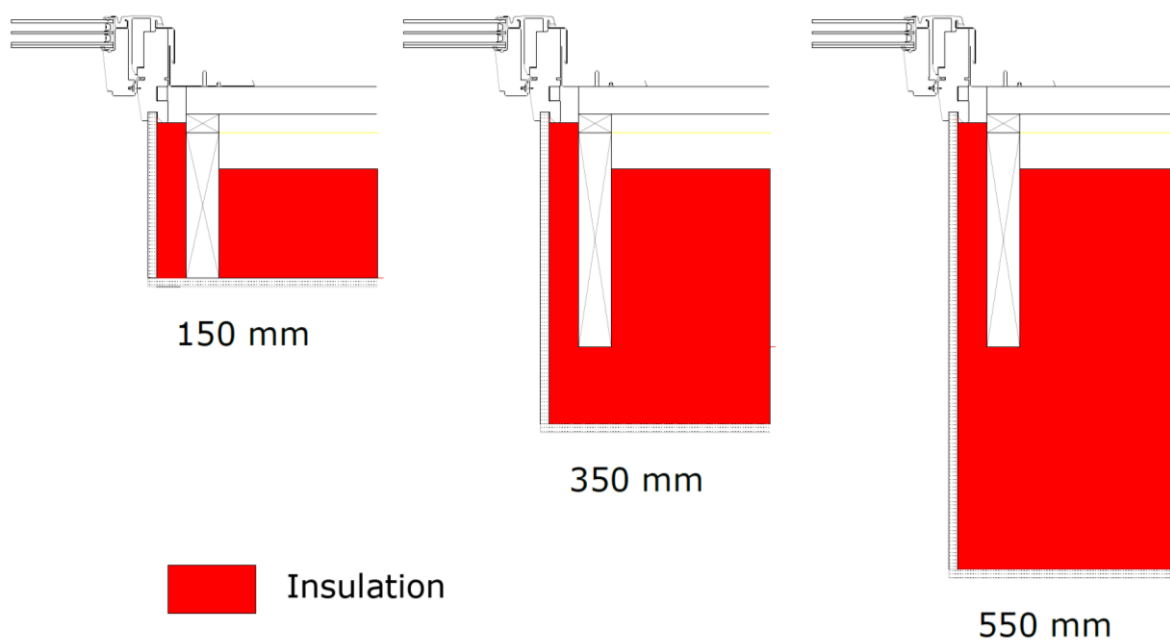
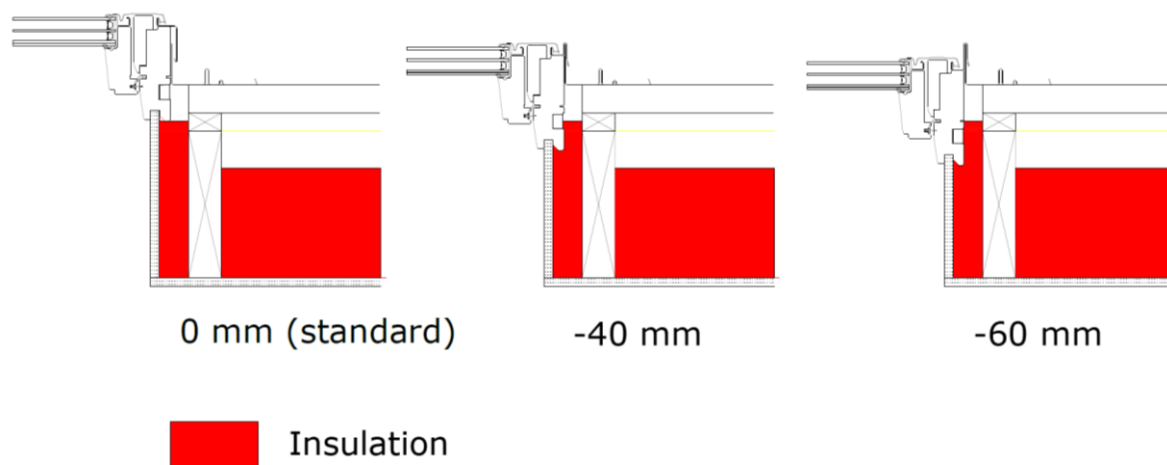**Figure 3: Cases of different insulation thicknesses.**

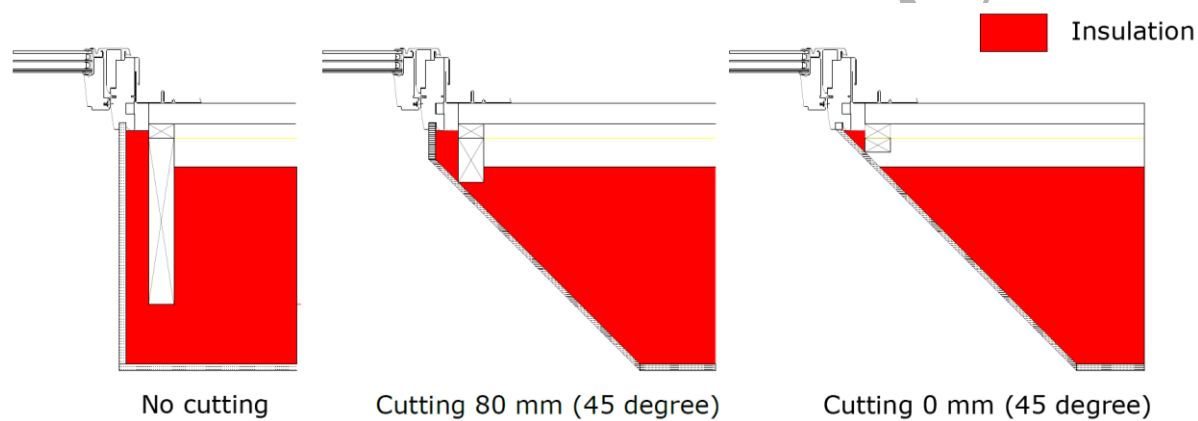**Figure 4: Cases of different positions of window installations.**

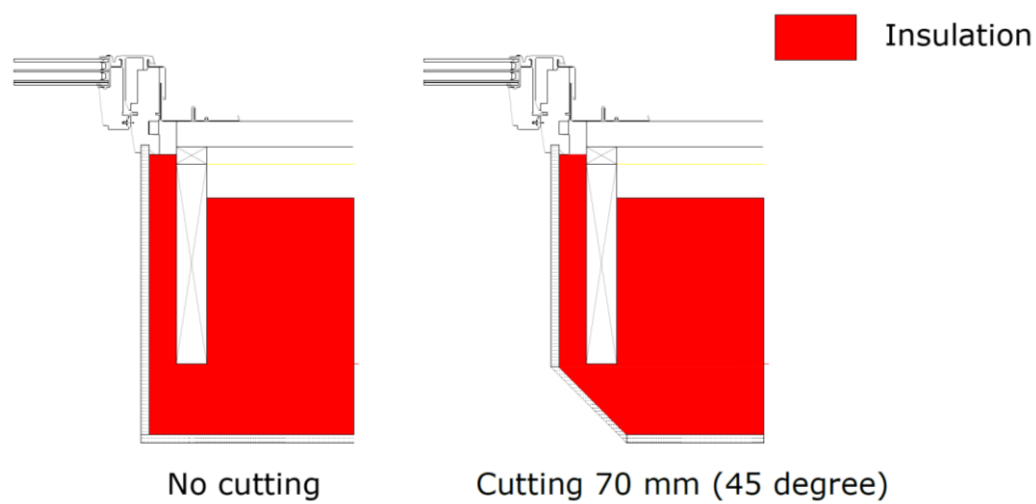**Figure 5: Different cases of cutting for the top and bottom lining.**

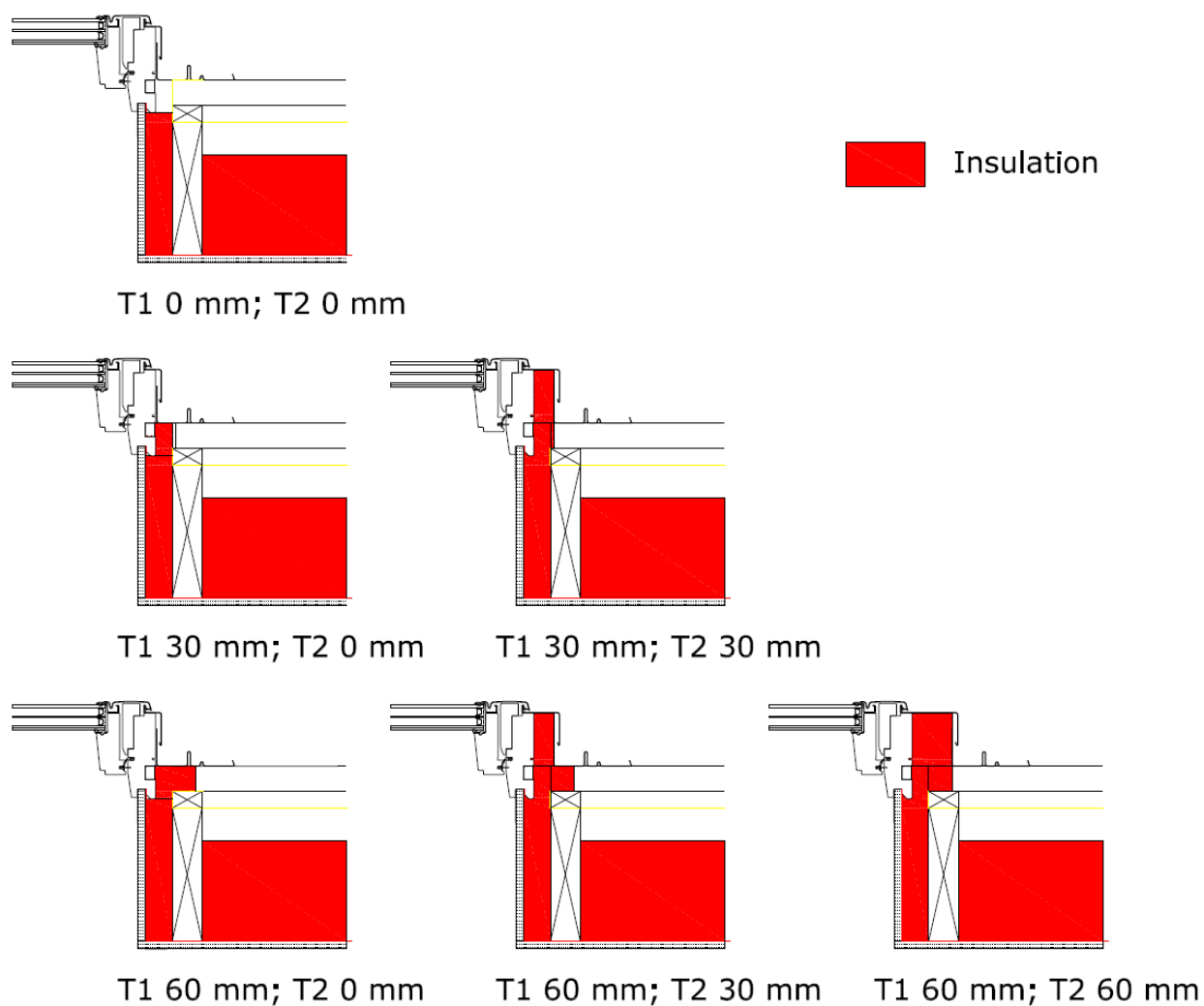**Figure 6: Cases of cutting for side lining.**

T1 0 mm; T2 0 mm

Insulation

T1 30 mm; T2 0 mm

T1 30 mm; T2 30 mm

T1 60 mm; T2 0 mm

T1 60 mm; T2 30 mm

T1 60 mm; T2 60 mm

Figure 7: Different cases of insulation around installation (T1: Horizontal thickness of the first layer of insulation next to window frame; T2: Horizontal thickness of the second layer of insulation next to window frame.).
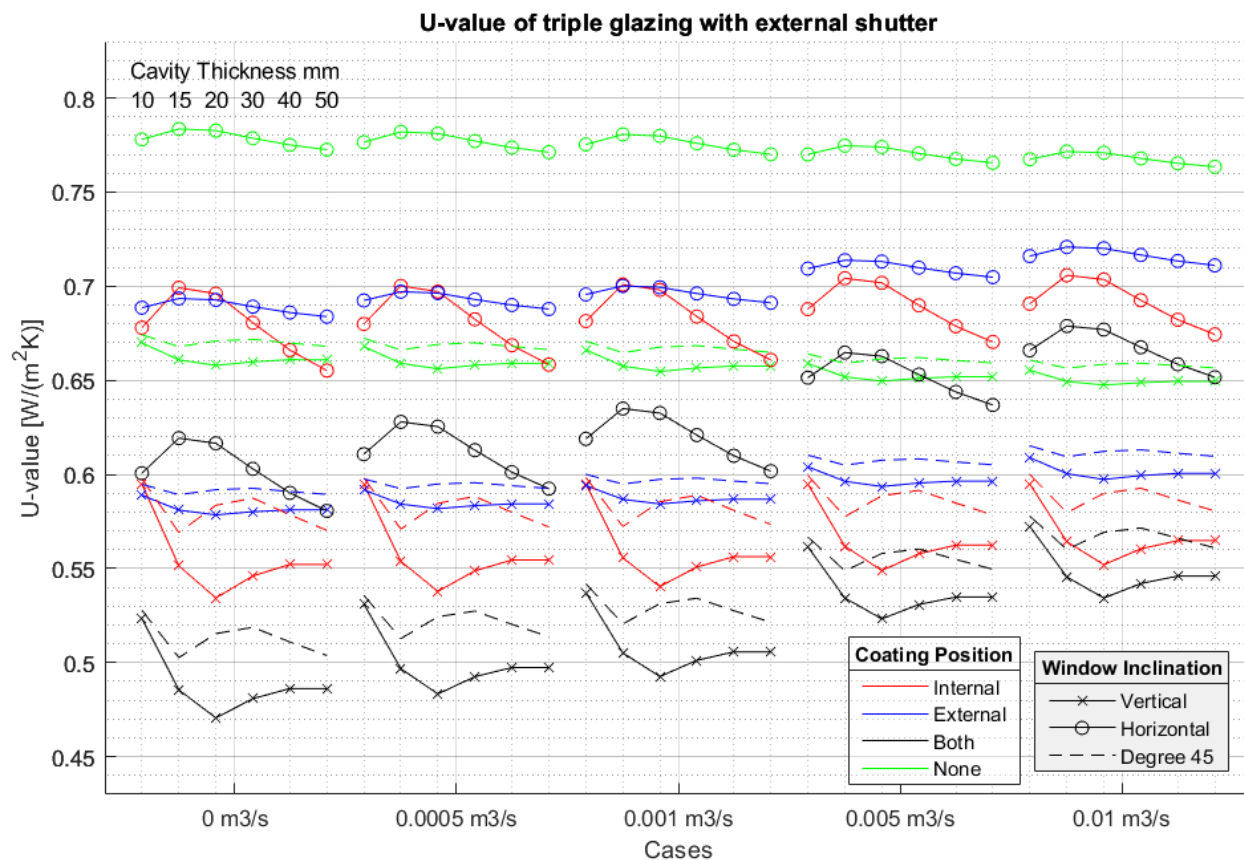
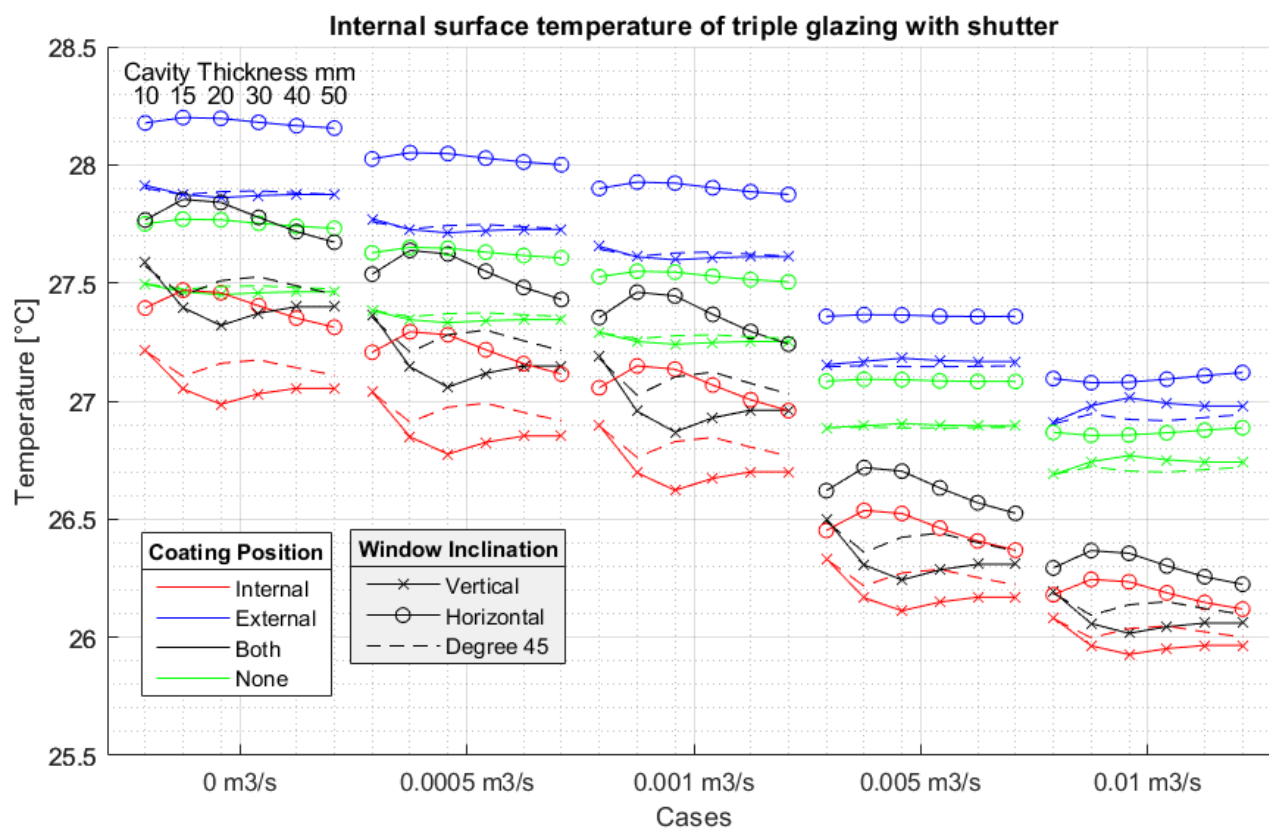**Figure 8: U-value of Triple glazing unit with external shutter.**

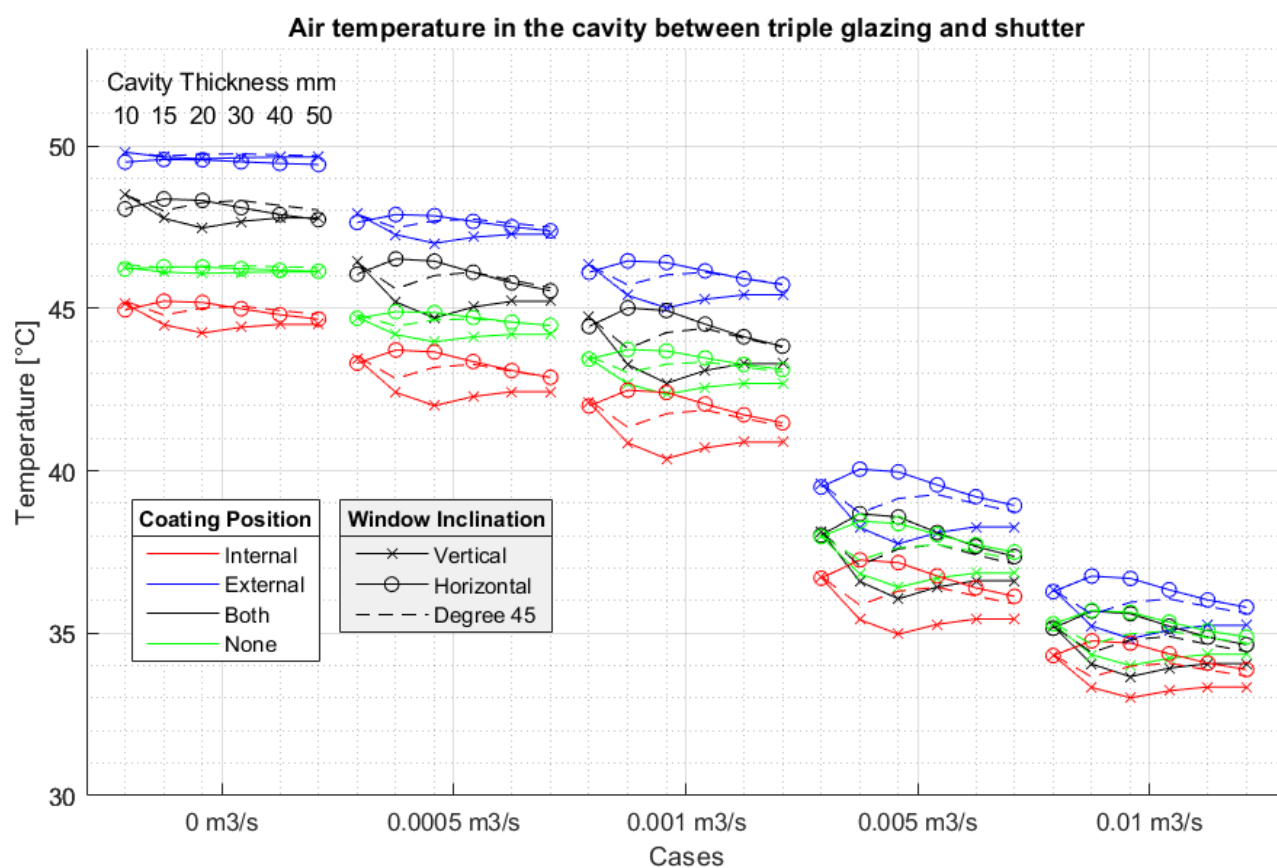**Figure 9: Surface temperature of the internal pane of triple glazing unit of different cases.**

Figure 10: Air temperature in the cavity between the triple glazing and shutter of different cases.
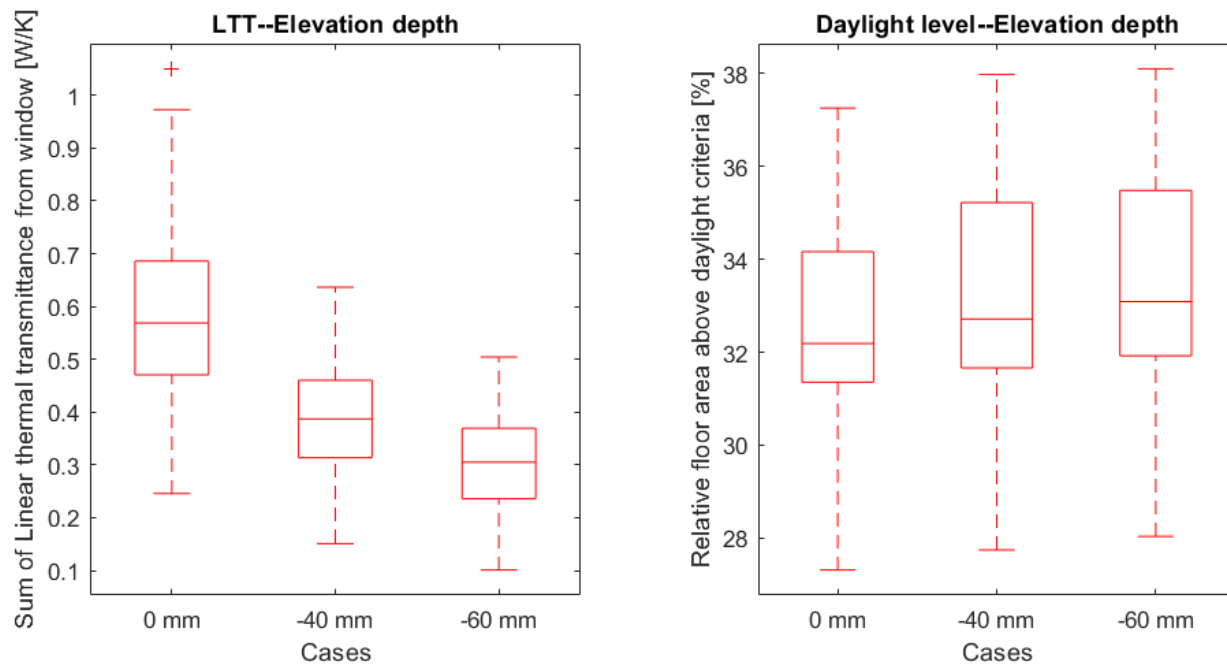
Figure 11: Daylight and thermal performance influenced by elevation depth of installation.
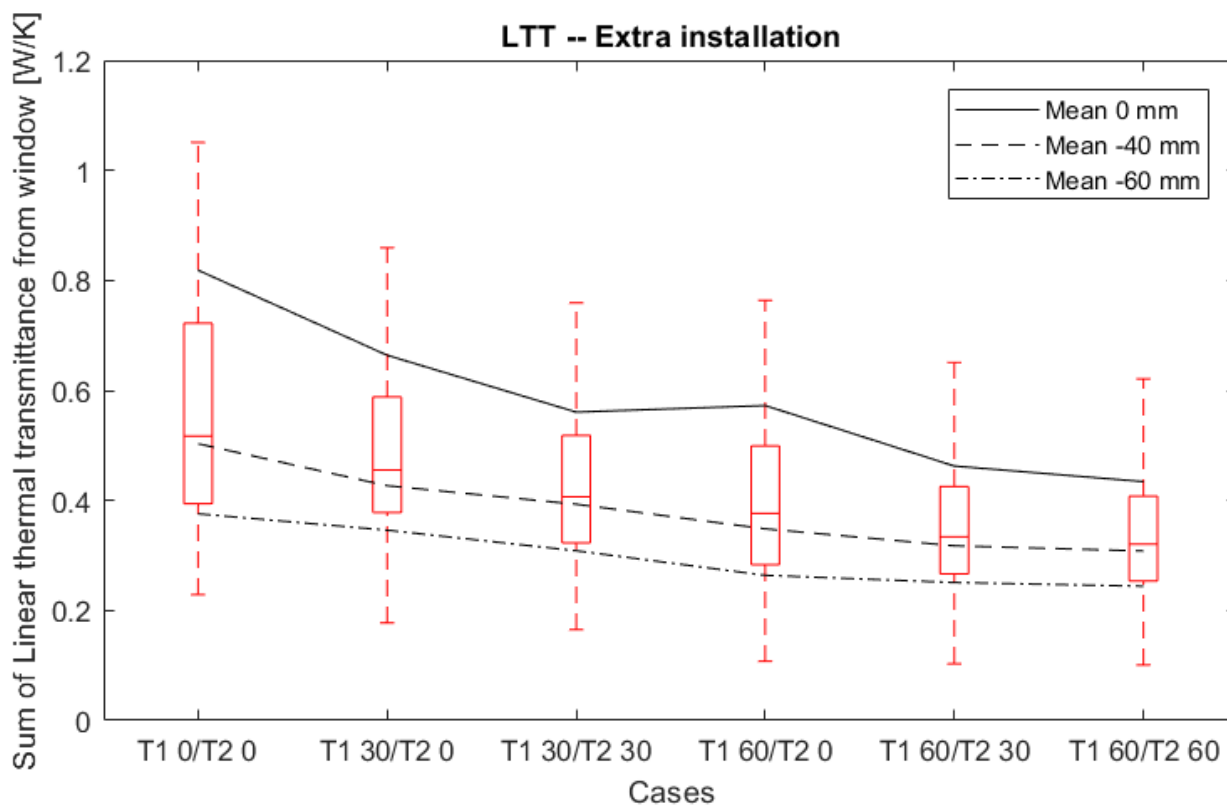

Figure 12: Thermal performance (LTT) influenced by extra insulation around the frame.
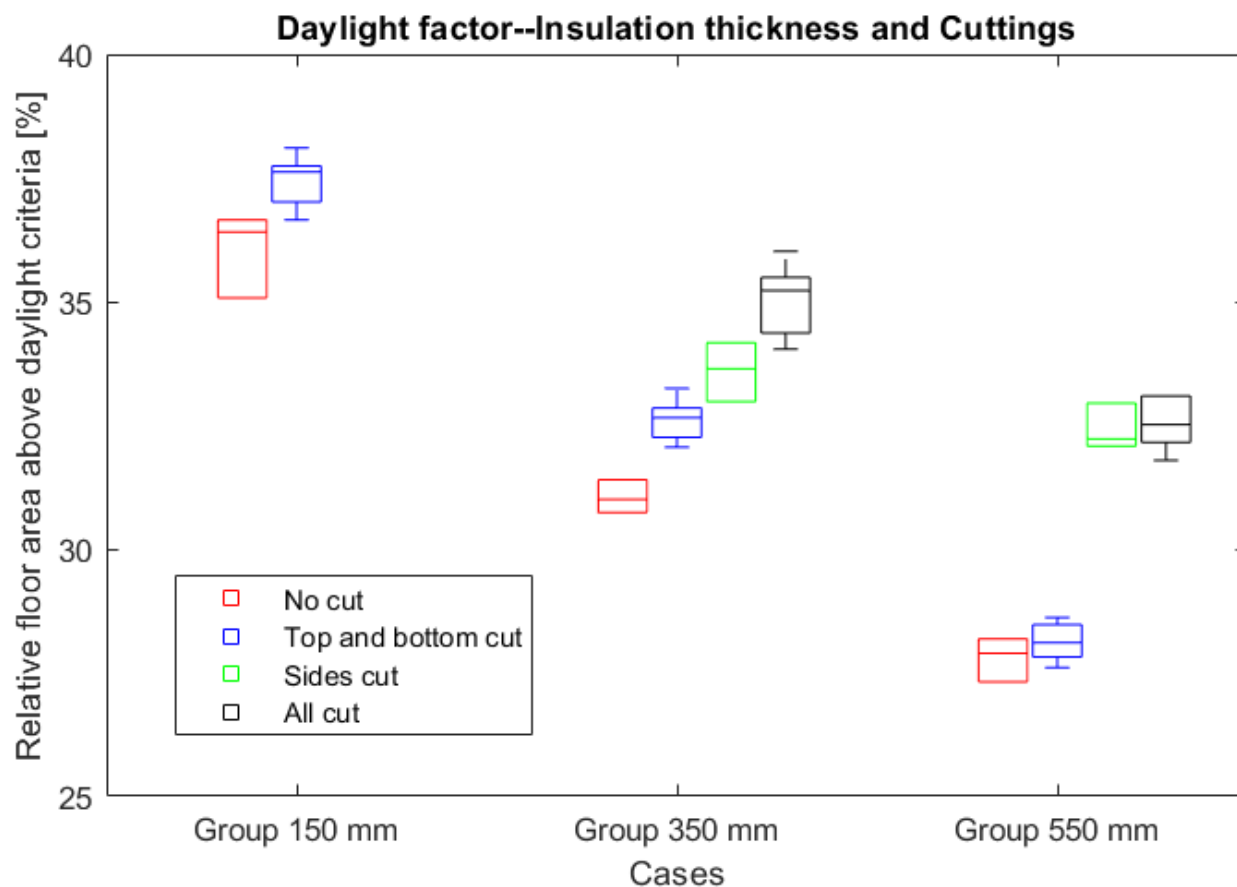
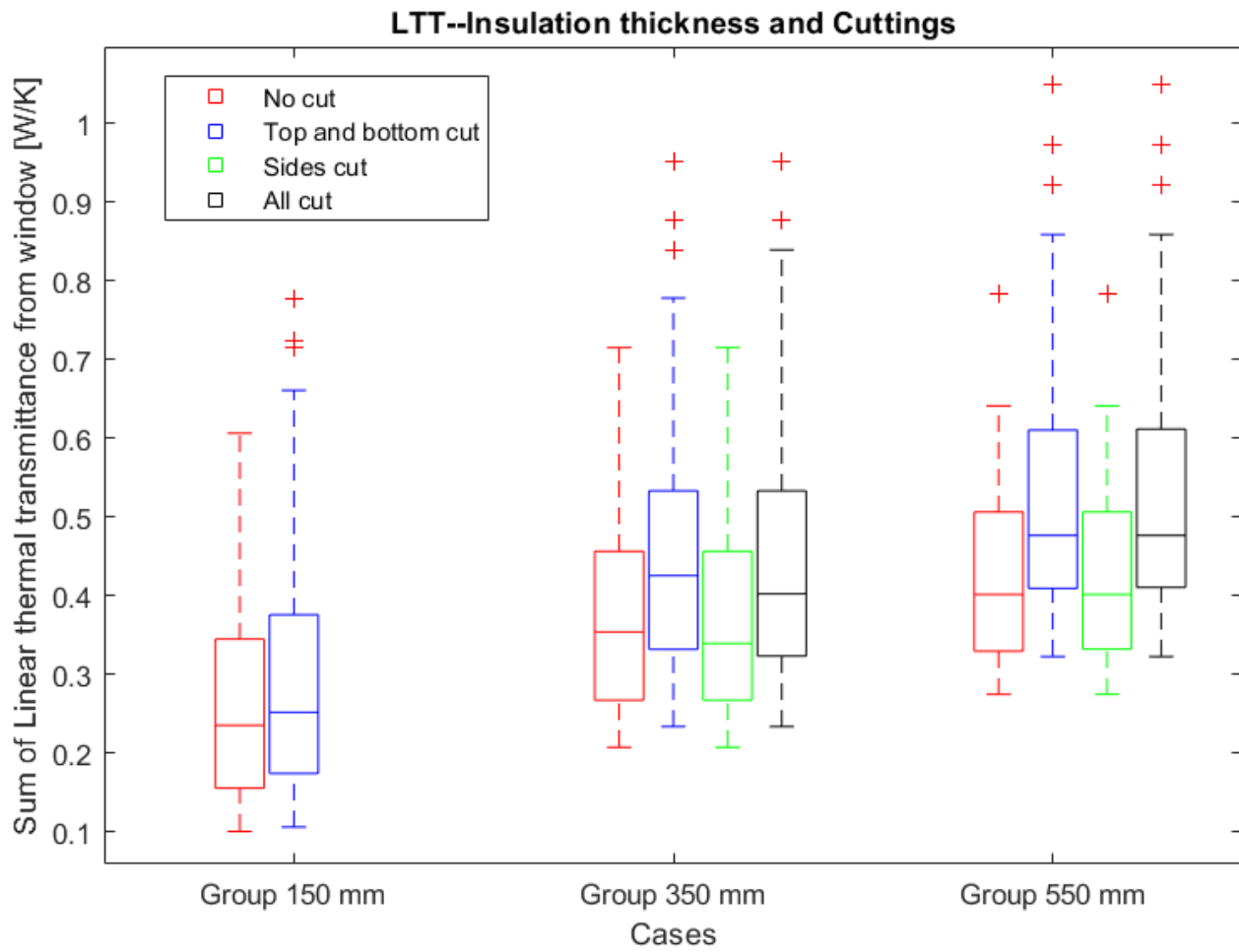**Figure 13: Daylight performance influenced by lining cuttings for different thicknesses of roof insulation.**

Figure 14: LTT influenced by lining cuttings for different thicknesses of roof insulation.

Table 1: Layout and properties of triple glazing unit used in the model.

Position	Material	Emissivity on external surface (E1) [-]	Emissivity on internal surface (E2) [-]	Solar transmittance (Tsol) [-]	Solar reflectance on external surface (Rsol1) [-]	Solar reflectance on internal surface (Rsol2) [-]	Heat conductivity [W/(mK)]
Outside	CLEAR 4T. KCC	0.837	0.837	0.808	0.076	0.076	1
Cavity	5% air and 95 % Argon 12 mm	-	-	-	-	-	-
Middle	PLANITHERM ONE	0.013	0.837	0.465	0.469	0.412	1
Cavity	5% air and 95 % Argon 12 mm	-	-	-	-	-	-
Inside	PLANITHERM UN 1	0.037	0.837	0.555	0.311	0.211	0.653

Table 2: Calculation parameters of triple glazing unit with external shutter.

Parameters	Value
Tilt angle of window with shutter	Vertical; Horizontal; 45 degree
Air penetration rate between cavity and outdoor air [m^3/s]	0; 0,0005; 0,001; 0,005; 0,01
Position of low-E coating on shutter, assumed emissivity of coating is 0.05	Without coating; Internal coating; External coating; Both
Thickness of cavity between shutter and glazing [mm]	10; 15; 20; 30; 40; 50

Table 3: Boundary conditions of winter and summer.

	Winter	Summer
Outdoor temperature (Tout) [°C]	0	30
Indoor temperature (Tin) [°C]	20	25
Solar radiation [W/m^2]	0	700

Table 4: Calculation parameters of different installation cases.

Parameters	Value
Roof thickness (mm)	150; 350; 550. (Figure 3)
Installation elevation of window (mm)	0 (standard); -40; -60. (Figure 4)
Cutting on top lining	0 mm (45 degrees); 80 mm (45 degrees); 90 degrees (no cutting). (Figure 5)
Cutting on bottom lining	0 mm (45 degrees); 80 mm (45 degrees); 90 degrees (no cutting). (Figure 5)
Cutting on side lining (only for the roof with the insulation of 350 mm and 550 mm)	0 mm (45 degrees); 90 degrees (no cutting). (Figure 6)
The first layer of insulation next to window frame (mm)	30; 60. (Figure 7)
The second layer of insulation next to window frame (mm)	30; 60. (Figure 7)